Development

Volume 127 (12) June 2000

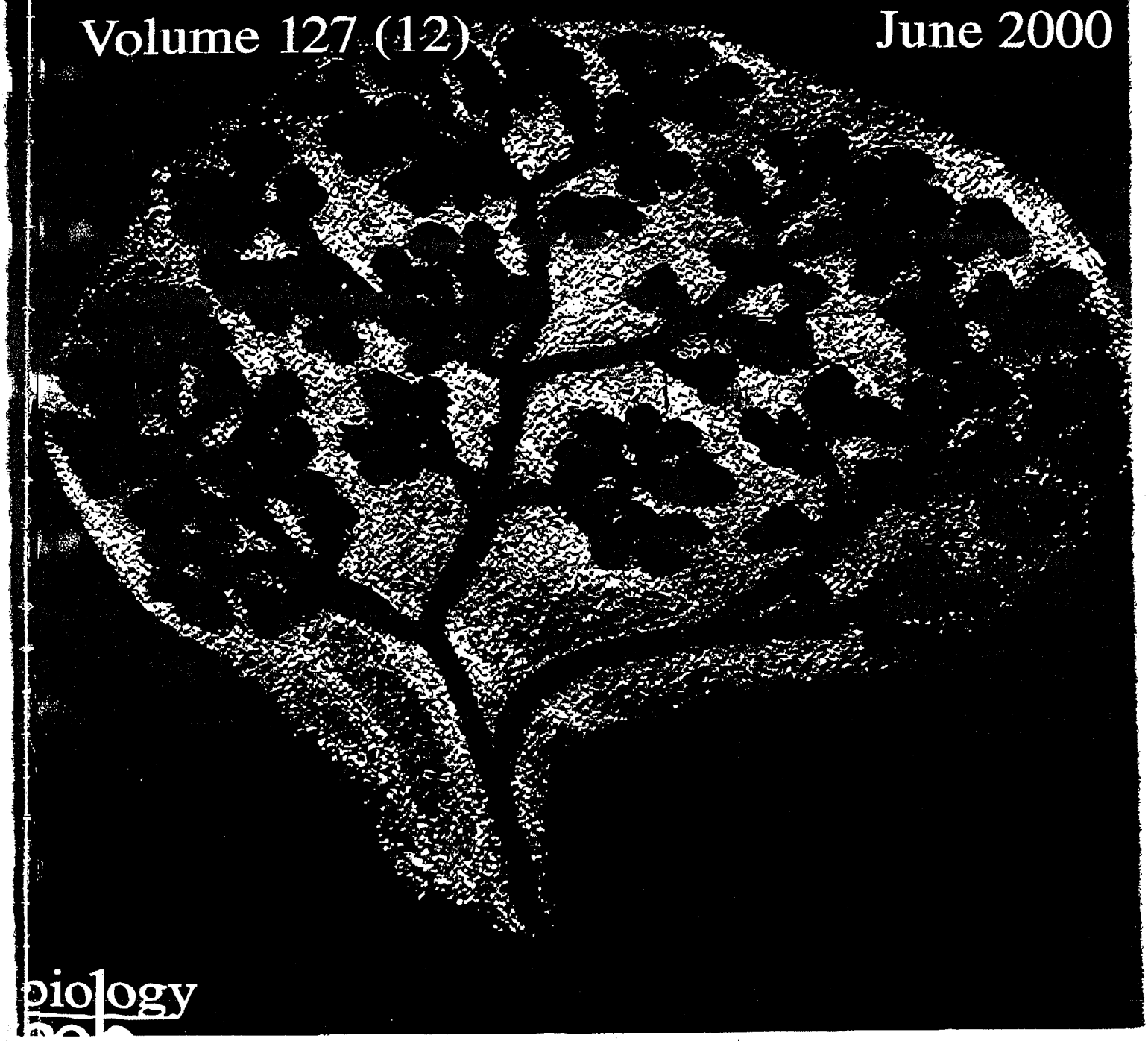

biology

Development

Contents

Volume 127 (12) 2000

Development 127, 2593-2606 (2000)
Printed in Great Britain © The Company of Biologists Limited 2000
DEV4389

Presenilin-1 regulates neuronal differentiation during neurogenesis

Melissa Handler*, Xudong Yang* and Jie Shen‡

Center for Neurologic Diseases, Department of Neurology, Brigham and Women's Hospital, Harvard Medical School, Boston, MA 02115, USA

*These authors contributed equally to the work

‡Author for correspondence (e-mail: jshen@cnd.bwh.harvard.edu)

Accepted 28 March; published on WWW 23 May 2000

SUMMARY

Mutations in *Presenilin-1* (*PS1*) are a major cause of familial Alzheimer's disease. Our previous studies showed that PS1 is required for murine neural development. Here we report that lack of PS1 leads to premature differentiation of neural progenitor cells, indicating a role for PS1 in a cell fate decision between postmitotic neurons and neural progenitor cells. Neural proliferation and apoptotic cell death during neurogenesis are unaltered in $PS1^{-/-}$ mice, suggesting that the reduction in the neural progenitor cells observed in the $PS1^{-/-}$ brain is due to premature differentiation of progenitor cells, rather than to increased apoptotic cell death or decreased cell proliferation. In addition, the premature neuronal differentiation in the $PS1^{-/-}$ brain is associated with aberrant neuronal migration and disorganization of the laminar architecture of the developing cerebral hemisphere. In the ventricular zone of $PS1^{-/-}$ mice, expression of the Notch1 downstream effector gene *Hes5* is reduced and expression of the Notch1 ligand *Dll1* is elevated, whereas expression of *Notch1* is unchanged. The level of *Dll1* transcripts is also increased in the presomitic mesoderm of $PS1^{-/-}$ embryos, while the level of *Notch1* transcripts is unchanged, in contrast to a previous report (Wong et al., 1997, *Nature* 387, 288-292). These results provide direct evidence that PS1 controls neuronal differentiation in association with the downregulation of Notch signalling during neurogenesis.

Key words: Alzheimer's disease, Hes5, Dll1, Notch1, Cell fate determination, Brain

INTRODUCTION

PS1 is a major gene responsible for familial Alzheimer's disease (FAD), and mutations in *PS1* account for approximately 50% of early-onset FAD cases (Selkoe, 1998). Understanding the normal physiological functions of PS1 may shed light on the pathogenic mechanism of FAD-linked PS1 mutations. Identification of the *PS1* homologue in *C. elegans*, *sel-12*, which facilitates signalling mediated by the Notch homologue LIN-12, provided the first evidence that PS1 interacts with the Notch signalling pathway (Levitan and Greenwald, 1995). The LIN-12/Notch family of receptors mediates cell-cell interactions that specify cell fate during development. SEL-12 affects LIN-12 activity by regulating its processing or trafficking (Levitan and Greenwald, 1998). PS1 shares functional homology with SEL-12, based on the finding that the wild-type human *PS1* cDNA complements the *sel-12* mutant phenotype (Baumeister et al., 1997; Levitan et al., 1996). However, PS1 containing FAD-linked mutations exhibited reduced ability to rescue *sel-12* mutations, suggesting that mutant PS1 has reduced biological activity (Baumeister et al., 1997; Levitan et al., 1996).

Recent identification of the *Drosophila Presenilin* (*PS*) provided further evidence for the interaction between PS1 and the Notch signalling pathway (Struhl and Greenwald, 1999; Ye et al., 1999). Fly mutants lacking both maternal and zygotic PS exhibit a neurogenic phenotype and are virtually indistinguishable from the *Notch*-null mutant, suggesting that PS function is required for normal Notch signalling in *Drosophila* (Struhl and Greenwald, 1999; Ye et al., 1999). PS is also required for the proteolytic cleavage of Notch to release its intracellular effector domain (ICD) (Struhl and Greenwald, 1999). The involvement of Presenilins in Notch processing is further supported by in vitro studies using truncated Notch1 and primary cell cultures derived from $PS1^{-/-}$ mice (De Strooper et al., 1999; Song et al., 1999). Levels of the ICD fragment were reduced in cultured $PS1^{-/-}$ neurons and fibroblasts, indicating that PS1 is important for the efficient proteolytic release of the ICD. PS1 bearing FAD-linked mutations exhibits reduced ability to rescue this Notch processing defect in cultured $PS1^{-/-}$ cells, suggesting that mutant PS1 has reduced activity in Notch processing (Song et al., 1999).

To characterize the normal physiological role of PS1 in mice, we previously generated mice with a targeted germ-line disruption of the *PS1* gene (Shen et al., 1997). Mutant mice homozygous for the resulting null allele exhibited similar defects in somitogenesis to those observed in *Notch1*-null mutant mice (Conlon et al., 1995; Swiatek et al., 1994), as well as severe malformation of the axial skeleton and cerebral hemorrhage (Shen et al., 1997; Wong et al., 1997). Furthermore, we showed that lack of PS1 results in a reduction

in the neural progenitor population and a subsequent reduction in the neuronal population, indicating a critical role for PS1 in murine neurogenesis (Shen et al., 1997). We also observed symmetric, region-specific loss of neural progenitor cells in the diencephalon and telencephalon of the *PS1*$^{-/-}$ brain beginning at E12.5 and 14.5, respectively. Loss of Cajal-Retzius neurons in late embryonic development has also been reported (Hartmann et al., 1999).

Here, we report that the reduction in the neural progenitor population in *PS1*$^{-/-}$ mice is caused by premature differentiation of neural progenitor cells. To investigate further the mechanism by which PS1 regulates neuronal differentiation, we examined the expression of genes involved in the Notch signalling pathway. We found a reduction in the level of *HES-5* transcripts as well as an increase in the level of *Dll1* transcripts in the *PS1*$^{-/-}$ brain, indicating that absence of PS1 function leads to reduced Notch signalling during neural development. We also found that expression of *Dll1* is increased in the presomitic mesoderm of *PS1*$^{-/-}$ embryos, whereas *Notch1* expression is unchanged, in contrast to a previous publication reporting that expression of both *Notch1* and *Dll1* is markedly reduced in the presomitic mesoderm of *PS1*$^{-/-}$ embryos (Wong et al., 1997). Taken together, our findings provide the first evidence that PS1 controls neuronal differentiation and the expression of the downstream target genes regulated by Notch signalling.

MATERIALS AND METHODS

Preparation of brain sections

Timed matings between heterozygous *PS1* knockout mice were set up, and the morning of the day when a vaginal plug is seen is designated as embryonic day 0.5 (E0.5). Embryos at the desired developmental stages were dissected from pregnant females, and the tail and limbs were removed from each embryo for genotyping. Embryonic heads were then removed and fixed in 4% paraformaldehyde for 2-3 hours at 4°C, cryoprotected overnight at 4°C in 30% sucrose, embedded in OCT medium (Tissue-Tek) and frozen on dry ice. Serial transverse sections (7-10 μm) were cut on a cryostat and collected on coated slides. Embryos with cerebral hemorrhages, regardless of the severity, were discarded.

Immunohistochemical analysis

Brain sections were blocked for 3 hours at room temperature with 3% nonfat milk, rinsed briefly in PBS and incubated overnight at 4°C with an anti-microtubule-associated protein 2 (MAP2) monoclonal antibody (1:1000, kindly provided by Dr Ken Kosik) or an anti-Nestin monoclonal antibody (1:1000, PharMingen). For Notch1 immunostaining, sections were incubated with a blocking solution containing 5% goat serum, 1% BSA, 0.1% glycine, 0.1% L-lysine and 0.4% Triton X-100 in PBS for 1 hour at room temperature followed by incubation with a polyclonal antibody (IC) against mouse Notch1 amino acid residues 1759-2306 (1:250, kindly provided by Dr Alan Israel) overnight at 4°C. Sections were then rinsed twice in PBS and incubated at room temperature with a rhodamine-conjugated goat anti-mouse secondary antibody (Jackson Immunoresearch) for MAP2 (1:400) and Nestin (1:100). For Notch1 immunostaining, the sections were rinsed three times in PBS and incubated with a fluorescein-conjugated goat anti-rabbit secondary antibody (1:500, Alexa) for 1 hour at room temperature. Images were viewed and collected on a Zeiss Axioscop connected with a SPOT 2 Cooled Color Digital camera (Diagnostic Instruments) or a BioRad MRC 1024 confocal laser scanning microscope.

BrdU labelling, immunodetection and quantification

Pregnant females were injected intraperitoneally with BrdU (10 mg/ml) at 100 μg/g body mass. After 30 minutes or 96 hours of labelling, embryos were removed, processed and serially sectioned. The brain sections were incubated in 2 N HCl for 1 hour at 37°C, neutralized in borate buffer (pH 8.5) for 1 hour at room temperature, rinsed twice in PBS and blocked with 3% nonfat milk for 3 hours at room temperature. The sections were then incubated with an anti-BrdU monoclonal antibody (1:10, Becton Dickinson) overnight at 4°C, rinsed twice in PBS, followed by incubation with a rhodamine-conjugated goat anti-mouse secondary antibody (1:100, Jackson Immunoresearch) for 1 hour at room temperature.

The percentage of BrdU-labelled cells was determined by dividing the number of BrdU$^+$ cells by the total number of progenitor cells. For both *PS1*$^{-/-}$ and littermate control brains, the number of BrdU$^+$ cells was counted in a comparable area of the anterior telencephalon and in half of the diencephalon. The total number of progenitor cells in the telencephalon was determined by counting the number of nuclei stained with Sytox Green in the comparable area on the adjacent sections, since there are few postmitotic neurons in the telencephalon at E10.5. Due to the presence of postmitotic neurons in the diencephalon at this stage, the total number of progenitor cells in the diencephalon was determined by subtracting the number of MAP2-positive cells from the total number of Sytox Green-stained cells in half of the diencephalon on the adjacent sections. A Zeiss Axioscop equipped with a reticular eyepiece was used to count the number of cells in an area of 5×10^4 μm^2 in the telencephalon and half of the diencephalon under 63× magnification.

Detection and quantification of apoptotic cells

The TUNEL (terminal-deoxynucleotidyl-transferase-mediated deoxyuridine triphosphate nick-end labelling) assay was used to label cells that are undergoing apoptosis. Brain sections were rinsed in PBS for 5 minutes and then 50-75 μl of TUNEL reaction mixture (In situ cell death detection kit, Boehringer Mannheim) was applied to each slide. The sections were incubated at 37°C for 1 hour and 15 minutes, rinsed twice in PBS and then incubated in bisbenzimide (2 μg/ml) for 10 minutes at room temperature. Apoptotic cells were identified by their TUNEL-reactivity as well as their fragmented and condensed nuclei stained by bisbenzimide. The number of apoptotic cells in each brain was quantified by counting three serial sections under 40× magnification. Statistical significance was determined by Student's *t*-test.

In situ hybridization

Sense and antisense riboprobes were synthesized using an in vitro transcription kit (Boehringer Mannheim) following the manufacturer's instructions and then hydrolyzed to approximately 100-200 nucleotides (nt) fragments. In situ hybridization was carried out as previously described (Schaeren-Wiemers and Gerfin-Moser, 1993) with minor modifications. Brain sections were incubated with the prehybridization solution (50% formamide, 5× SSC, 0.02% SDS, 0.1% N-lauroylsarcosine and 2% blocking reagent) at room temperature (RT) for 6 hours, then hybridized together in hydrolyzed riboprobes (40 ng/ml) at 70°C overnight.

For color detection, the sections were placed upside down on NBT/BCIP reaction mixture containing 2 mM freshly prepared levamisole. The slides containing brain sections were elevated with two spacers (0.2 mm) to allow sufficient and equal contact with the reaction mixture. Precautions were taken to ensure identical conditions for all procedures of in situ hybridization involving the *PS1*$^{-/-}$ and littermate control brain sections. All images were collected with a cooled CCD camera with identical exposure time between the

PS1$^{-/-}$ and control brain sections. The brain sections hybridized with the sense probe showed no staining.

Northern analysis

Heads and tail buds from *PS1*$^{-/-}$ and littermate control mice at E11.5 were collected for the preparation of total RNA using Tri Reagent (Sigma). Poly(A)Pure kit (Ambion) was used to enrich poly(A)$^+$ RNA from total RNA. Approximately 30 μg of total RNA and 5 μg of poly(A)$^+$ RNA were used for the Northern blotting. The blots were hybridized with ^{32}P-labelled probes, which were synthesized with Prime-It II random labelling kit (Stratagene), in the hybridization solution (1% SDS, 6× SSC and 10% dextran sulfate) at 67°C overnight. The same blot was then hybridized with a *G3PDH* probe to normalize the amounts of mRNA loaded in each lane. NIH Image software was used to quantify the level of transcripts by comparing the intensities of the bands after subtracting the background.

Quantification of *Dll1*-expressing cells

In situ hybridization was performed on comparable sections from *PS1*$^{-/-}$ and littermate control brains at E11.5 under identical conditions. The images of brain sections and a micro-ruler were collected with a CCD camera under the same magnification and resolution. The large number of *Dll1*-expressing cells in the diencephalon, particularly in the *PS1*$^{-/-}$ diencephalon, makes it difficult to count the number of *Dll1*$^+$ cells accurately in the diencephalon; therefore, our analysis was focused on the telencephalon. *Dll1*-positive cells in half of the telencephalon were counted on the collected brain sections, and the area of half of the telencephalon was measured using NIH Image software. The density of *Dll1*-expressing cells was calculated by dividing the number of *Dll*$^+$ cells by the measured area. The data shown represent an average of one section from three brains per genotype.

Whole-mount in situ hybridization

Whole-mount in situ hybridization was performed essentially as described (Hogan et al., 1994). Briefly, embryos at day 9.5 were dissected and fixed in 4% paraformaldehyde at 4°C overnight. Yolk sacs were used for genotyping. After genotyping, *PS1*$^{-/-}$ and littermate control (*PS1*$^{+/-}$) embryos were processed either individually or together during subsequent steps. The same probes were used as those used for in situ hybridization on brain sections. For those embryos that were processed together, the *PS1*$^{-/-}$ and control embryos were later identified by the morphological differences in somites (Shen et al., 1997).

RESULTS

To understand the normal function of PS1 in the brain, we examined the *PS1*$^{-/-}$ embryonic brain for defects in neural development. Beginning at embryonic day 12.5 (E12.5), it becomes evident that the ventricular zone in the *PS1*$^{-/-}$ brain is thinner than in the control brain, reflecting a reduction in the population of neural progenitor cells during neurogenesis (Shen et al., 1997). Cortical neurogenesis in mice begins at approximately E11 and continues through E17, comprising 11 cell cycles (McConnell, 1995; Takahashi et al., 1995). During early neurogenesis, very few progenitor cells in the neuroepithelium exit the cell cycle to become postmitotic neurons, while the vast majority of progenitor cells reenter the cell cycle after mitosis, resulting in a steady expansion of the neural progenitor population. As neurogenesis progresses, a fraction of neural progenitor cells exit the cell cycle, differentiate into postmitotic neurons and migrate to form the developing neocortex. Therefore, a reduction in the population of neural progenitor cells could occur *via* several possible mechanisms: premature differentiation of progenitor cells, decreased proliferation, or increased apoptotic cell death. To distinguish among these possibilities, we compared the *PS1*$^{-/-}$ and control brains for differences in neuronal differentiation and migration, cell proliferation and survival. Due to severe cerebral hemorrhage often associated with *PS1*$^{-/-}$ mice at later embryonic stages, our analysis is focused on the examination of the *PS1*$^{-/-}$ and control brains that are free of hemorrhages between E10.5 and 13.5.

Premature differentiation of neural progenitor cells in *PS1*$^{-/-}$ mice

To assess neuronal differentiation in the *PS1*$^{-/-}$ and control brains, we performed immunostaining for MAP2, a marker specific for postmitotic neurons (Crandall et al., 1986). Serial transverse sections of the *PS1*$^{-/-}$ and littermate control brains at E10.5, 11.5, 12.5 and 13.5 were stained with anti-MAP2 antibody, and corresponding sections of the *PS1*$^{-/-}$ and control brains were compared. Although few MAP2-immunoreactive neurons are present in the telencephalon at E10.5 (data not shown), as many as 4-6 layers of MAP2$^+$ neurons were detected in the *PS1*$^{-/-}$ diencephalon, whereas only 1-2 layers of MAP2$^+$ neurons were detected in the control (Fig. 1A). The ratio of MAP2$^+$ cells to total cell population in the *PS1*$^{-/-}$ diencephalon is two- to threefold higher than in the littermate control (data not shown).

At E11.5, increases in MAP2 immunoreactivity in the *PS1*$^{-/-}$ brain relative to the control are found in the anterior telencephalon (Fig. 1Ba,b), and more substantially in the posterior telencephalon (Fig. 1Bc,d). In the anterior telencephalon, 2-4 layers of MAP2$^+$ neurons were detected in the *PS1*$^{-/-}$ brain in comparison to a single layer of MAP2 immunoreactive neurons in the littermate control (Fig. 1Ba,b). The ventricular zone in this region contains similar numbers of MAP2-negative progenitor cell layers in the *PS1*$^{-/-}$ brain and the control. The posterior telencephalon of the *PS1*$^{-/-}$ brain contains more layers of MAP2$^+$ neurons and a smaller ventricular zone in comparison to the control (Fig. 1Bc,d). The diencephalon exhibits the most substantial differences in the populations of MAP2-immunoreactive neurons and MAP2-negative progenitor cells. In the diencephalon of the *PS1*$^{-/-}$ brain, the MAP2-immunoreactive neurons encompass numerous cell layers and have largely replaced the MAP2-negative progenitor cells in the ventricular zone (Fig. 1Be-h).

At E12.5, these differences are still prominent in the telencephalon and diencephalon. More layers of MAP2$^+$ neurons are present in the anterior telencephalon in the *PS1*$^{-/-}$ brain (Fig. 1Ca,b), and the diencephalic ventricular zone is largely replaced by the MAP2$^+$ neurons (Fig. 1Cc,f). By E13.5, however, MAP2 immunoreactive neurons comprise a similar number of cell layers in the anterior telencephalon of the *PS1*$^{-/-}$ and littermate control brains (Fig. 1Da,b).

In summary, markedly increased numbers of postmitotic neurons identified by MAP2 immunoreactivity accumulate in the telencephalon and diencephalon of the *PS1*$^{-/-}$ brain during early neural development, accompanied by a progressive reduction in size of the ventricular zone. These observations indicate that neural progenitor cells differentiate into postmitotic neurons prematurely in the absence of PS1, resulting in early depletion of the neural progenitor population.

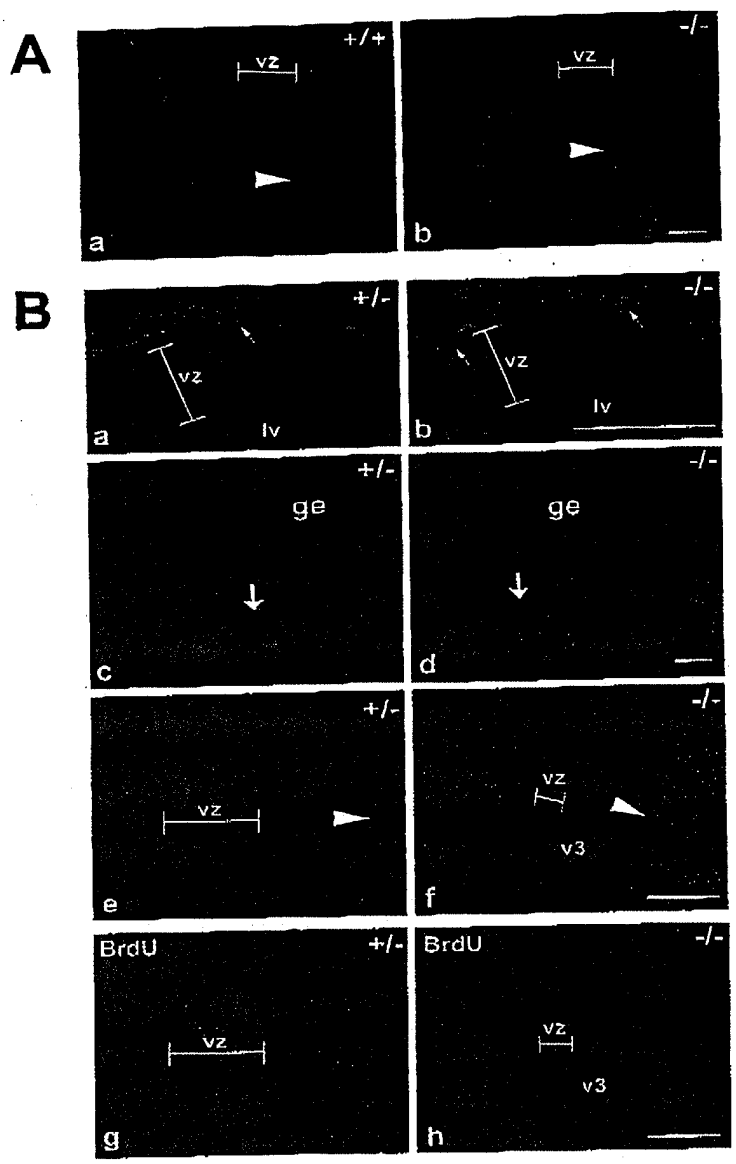

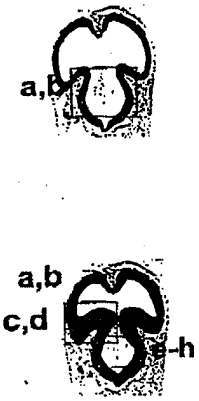

Fig. 1. Increased neuronal differentiation in the *PS1*$^{-/-}$ brain. Serial transverse brain sections (10 μm for E10.5 and 11.5, 7 μm for E12.5 and 13.5) of *PS1*$^{-/-}$ and littermate controls were stained with a monoclonal antibody directed against MAP2. Schematic diagrams of transverse views of the telencephalon and diencephalon are included to indicate the positions of brain subregions shown in the panels. At E10.5 (A) more MAP2 immunoreactive neurons are detected in the *PS1*$^{-/-}$ diencephalon compared to the littermate control (arrowheads in a and b). At E11.5 (B), an increased number of MAP2^{+} neurons are present in the telencephalon (small arrows in a and b), and more substantially in the ganglionic eminence (ge; large arrows in c and d) and diencephalon, where the difference is most striking (arrowheads in e and f). The ventricular zone (vz), which consists of MAP2 negative cells and is indicated by bars, is similar in size in the anterior telencephalon (a and b) but considerably thinner in the diencephalon (e and f) of the *PS1*$^{-/-}$ brain. BrdU-labelled cells are shown residing within the ventricular zone in the diencephalon (g and h). At E12.5 (C), there are more MAP2^{+} neurons in the anterior telencephalon of the *PS1*$^{-/-}$ brain (a and b). Nestin immunostaining is used to label neural progenitor cells in the neuroepithelium (c and d). A significant increase in the number of MAP2^{+} cells and a reduction in the ventricular zone are detected in the *PS1*$^{-/-}$ diencephalon (e and f). By E13.5 (D), the number of MAP2^{+} cell layers in the anterior telencephalon of the *PS1*$^{-/-}$ and control brains becomes similar (a and b), which could be explained by reduced neurogenesis in the *PS1*$^{-/-}$ brain due to a reduction in the progenitor population at this embryonic stage. More postmitotic neurons are generated in the control brain between E12.5 and 13.5, compensating for the smaller neuronal population at E12.5. lv, lateral ventricles; v3, third ventricle. Bars, 100 μm.

Interestingly, the severity of this phenotype varies in the brain subregions examined. The diencephalon exhibits the most striking difference in MAP2 immunoreactivity, whereas the anterior telencephalon shows the least difference. Thus, during neurogenesis, PS1 controls neuronal differentiation in a region-specific manner by regulating the cell-fate choice between neural progenitor cells and postmitotic neurons.

The role of PS1 in proliferation of neural progenitor cells

Although premature neuronal differentiation provides an explanation for the reduction in the number of neural progenitor cells observed in the *PS1*$^{-/-}$ brain, it remained possible that a decrease in cell proliferation and/or an increase in apoptotic cell death could be contributing factors as well. Cell proliferation in the neuroepithelium was examined by BrdU labelling. The fraction of cells labelled with BrdU during a short pulse reflects the fraction of cells in S phase during that period, permitting an assessment of the proliferation rate of a population of cells (Gratzner, 1982). After 30 minutes of BrdU pulse-labelling, serial transverse sections of the *PS1*$^{-/-}$ and littermate control brains were stained with anti-BrdU antibody. Comparable sections of the *PS1*$^{-/-}$ brains at E10.5, 11.5, 12.5 and 13.5 were compared to their littermate controls.

We observed no significant differences in the BrdU labelling patterns of the *PS1*$^{-/-}$ and littermate control brains at E10.5 (Fig. 2A). The ratio of BrdU-labelled cells to the total number of progenitor cells in the ventricular zone of the telencephalon and diencephalon is similar in the *PS1*$^{-/-}$ and control brains (Table 1). This result shows that lack of PS1 does not lead to a reduction in the proliferation rate of neural progenitor cells.

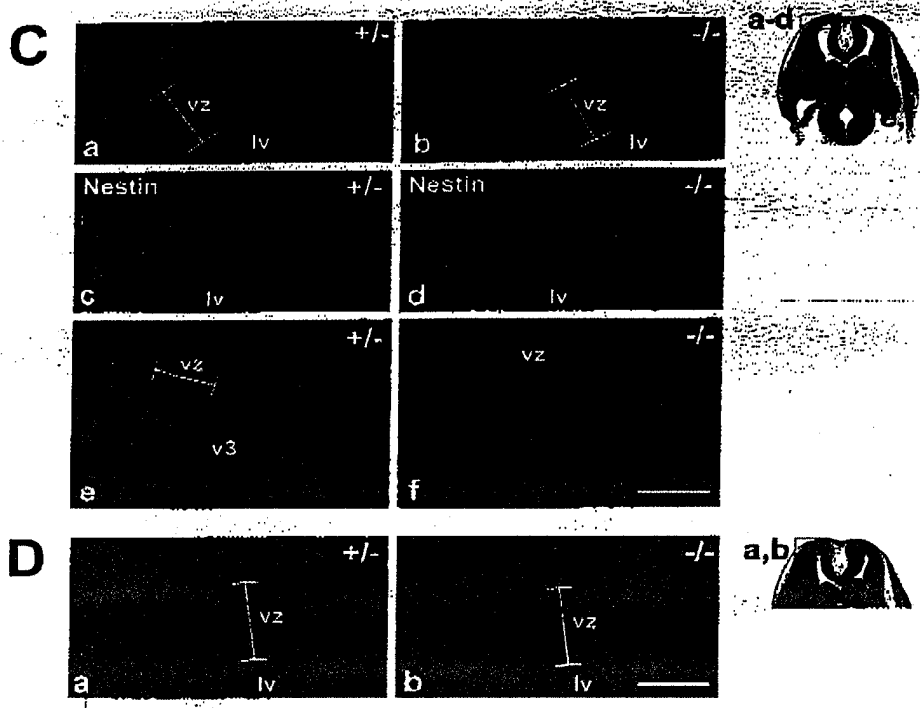

We did, however, observe differences in BrdU labelling in the diencephalon at E11.5. The BrdU labelling pattern in the telencephalon of the *PS1*$^{-/-}$ brain appears similar to that of the control (Fig. 2Ba,b), but fewer BrdU-labelled cells are detected in the diencephalon of the *PS1*$^{-/-}$ brain (Fig. 2Bc-f). The location of these BrdU-labelled cells in the *PS1*$^{-/-}$ brain corresponds to the thin remnant of the diencephalic ventricular zone revealed by the absence of MAP2 immunostaining at this age (Fig. 2Be,f; compare with unstained cells in Fig. 1Be,f). The BrdU labelling patterns of the anterior telencephalon are indistinguishable at E12.5 (Fig. 2Ca,b) and E13.5 (Fig. 2Da,b), but fewer BrdU-labelled cells appear to be present in the ganglionic eminence of the *PS1*$^{-/-}$ brain (Fig. 2Cc,d). The simplest explanation for the reduced BrdU labelling in the ganglionic eminence and diencephalon of the *PS1*$^{-/-}$ brain is that it is a secondary effect, reflecting early and progressive depletion of progenitor population in the ventricular zone of these brain regions due to premature differentiation of neural progenitor cells. The corresponding presence of increased numbers of postmitotic neurons in these particular regions supports this explanation.

Table 1. Comparison of BrdU labelling in the *PS1*$^{-/-}$ and control brains at E10.5

	Percentage of BrdU-labelled cells Control	Percentage of BrdU-labelled cells *PS1*$^{-/-}$
Telencephalon	83.6±12.4	82.3±12.6
Diencephalon	80.4±7.1	75.3±1.1

The percentage of BrdU-labelled cells was determined by dividing the number of BrdU-positive cells by the total number of neural progenitor cells. The data shown represent an average of 1-2 sections from 2-3 brains per genotype. Values are means ± s.d.

The role of PS1 in apoptotic cell death during early neurogenesis

To determine whether increased apoptotic cell death might contribute to the reduction in the neural progenitor population observed in the *PS1*$^{-/-}$ brain, we assessed the number of apoptotic cells in the *PS1*$^{-/-}$ and control brains at E11.5 and E12.5. Apoptotic cells were detected by the TUNEL assay, which labels the 3′-OH termini of DNA strand breaks generated during DNA fragmentation (Gavrieli et al., 1992). Bisbenzimide staining was also used to confirm the identity of apoptotic cells, which contain condensed, clumped and/or fragmented nuclei (Deckwerth and Johnson, 1993). Similar numbers of apoptotic cells labelled by the TUNEL assay were detected in the telencephalon (Fig. 3) and diencephalon (data not shown) of the *PS1*$^{-/-}$ and littermate control brains at E11.5 (Fig. 3a,b) and E12.5 (Fig. 3c,d).

Quantitative comparison of the number of apoptotic cells in multiple comparable sections of the *PS1*$^{-/-}$ and littermate control brains at E11.5 and E12.5 revealed no significant differences (Table 2). A total of 42-50 apoptotic cells were detected in transverse sections of the entire telencephalon and diencephalon of both *PS1*$^{-/-}$ and control brains. In addition, the small percentages of apoptotic cells (approx. 0.6% for E11.5 and 0.3% for E12.5) cannot account for the marked reduction of the progenitor population in the *PS1*$^{-/-}$ brain. Likewise, no significant differences in the number of apoptotic cells were seen in cultured primary neural progenitor cells derived from the *PS1*$^{-/-}$ and littermate control telencephalons at E12.5 (data not shown). These results indicate that increased apoptosis is not a primary cause of the defective neurogenesis in *PS1*$^{-/-}$ brain, and that PS1 is not involved in the regulation of apoptosis during early neurogenesis.

The role of PS1 in neuronal migration during early neural development

The laminar architecture of the developing cerebral hemisphere

Table 2. Comparison of apoptosis in the *PS1*$^{-/-}$ and control brains

Embryonic stage	Genotype	Number of apoptotic cells
E11.5	+/–	50±9
	–/–	47±5
E12.5	+/+	42±3
	–/–	44±6

For each genotype, the number of apoptotic cells represents an average of TUNEL-positive cells in the telencephalon and diencephalon of 2-3 adjacent sections per brain (n=3-5 brains). Values are means ± s.d.

There is no significant difference in the numbers of apoptotic cells in the *PS1*$^{-/-}$ and control brains at E11.5 (P=0.68) and E12.5 (P=0.54).

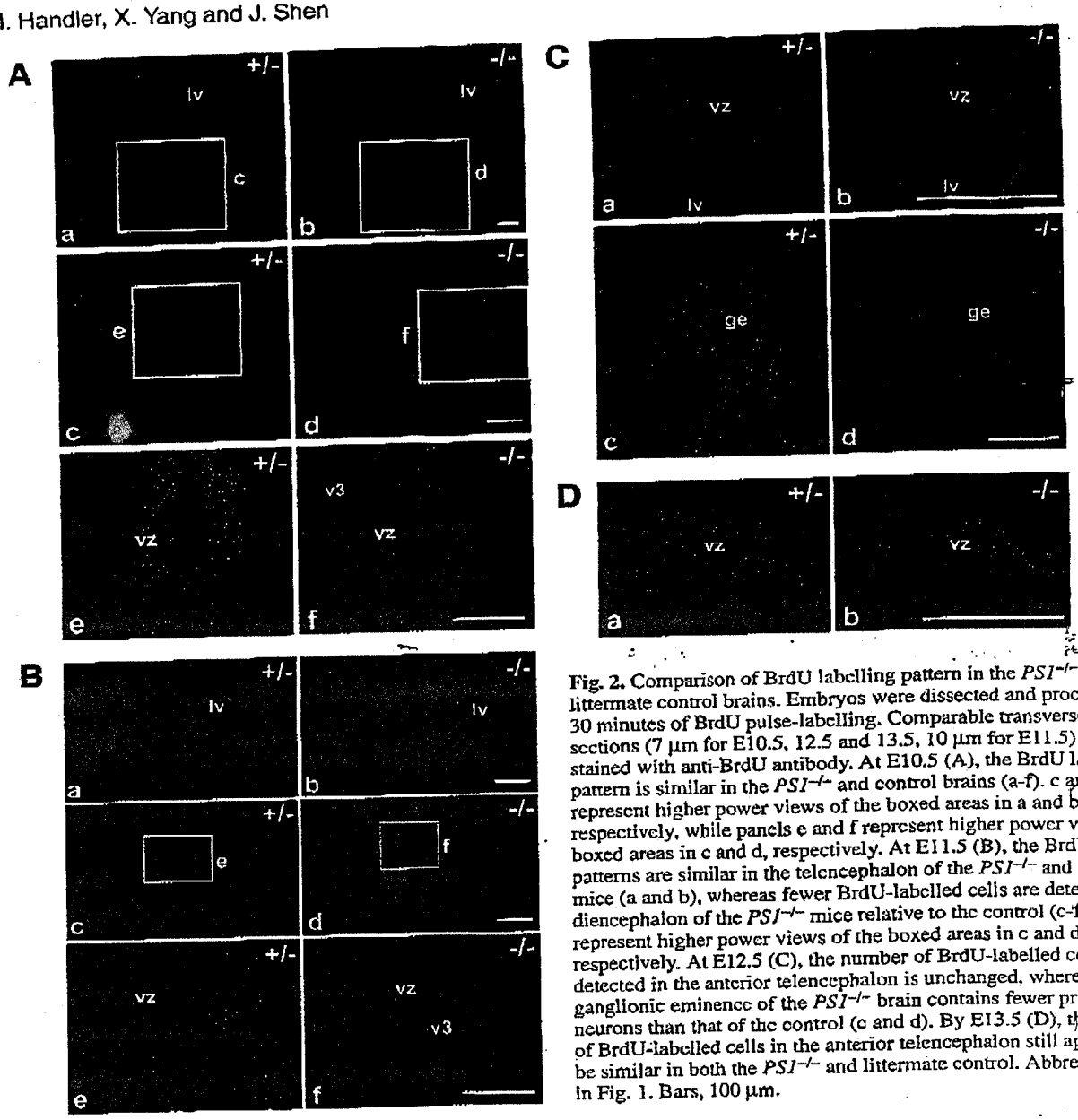

Fig. 2. Comparison of BrdU labelling pattern in the *PS1*$^{-/-}$ and littermate control brains. Embryos were dissected and processed after 30 minutes of BrdU pulse-labelling. Comparable transverse brain sections (7 μm for E10.5, 12.5 and 13.5, 10 μm for E11.5) were stained with anti-BrdU antibody. At E10.5 (A), the BrdU labelling pattern is similar in the *PS1*$^{-/-}$ and control brains (a-f). c and d represent higher power views of the boxed areas in a and b, respectively, while panels e and f represent higher power views of the boxed areas in c and d, respectively. At E11.5 (B), the BrdU labelling patterns are similar in the telencephalon of the *PS1*$^{-/-}$ and control mice (a and b), whereas fewer BrdU-labelled cells are detected in the diencephalon of the *PS1*$^{-/-}$ mice relative to the control (c-f). e and f represent higher power views of the boxed areas in c and d, respectively. At E12.5 (C), the number of BrdU-labelled cells detected in the anterior telencephalon is unchanged, whereas the ganglionic eminence of the *PS1*$^{-/-}$ brain contains fewer proliferating neurons than that of the control (c and d). By E13.5 (D), the number of BrdU-labelled cells in the anterior telencephalon still appears to be similar in both the *PS1*$^{-/-}$ and littermate control. Abbreviations as in Fig. 1. Bars, 100 μm.

is disrupted in the *PS1*$^{-/-}$ brain, as indicated by the absence of the characteristic demarcations among the developing cortical plate, the intermediate zone, the ventricular and subventricular zones in the *PS1*$^{-/-}$ brain at E14.5 (Fig. 4b). The cortical plate in particular appears poorly defined and generally thinner in the *PS1*$^{-/-}$ brain (Fig. 4b), compared to wild type (Fig. 4a) (Shen et al., 1997). In addition, occasional neuronal heterotopias are present in the marginal zone of the developing cortex in the *PS1*$^{-/-}$ brain at E17.5 (data not shown), as previously reported (Hartmann et al., 1999). These results indicate that cortical neuronal migration is abnormal in the *PS1*$^{-/-}$ brain.

To investigate further the pattern of cortical neuronal migration in *PS1*$^{-/-}$ mice, we pulse-labelled newly generated progenitor cells and neurons with BrdU at E10.5 and analyzed their migration pattern at E14.5. Comparison of corresponding transverse sections of the *PS1*$^{-/-}$ brain (Fig. 4d) and the littermate control (Fig. 4c) revealed an increased number of brightly stained cells in the *PS1*$^{-/-}$ telencephalon (Fig. 4d). These brightly stained cells represent differentiated neurons that exited the cell cycle immediately following the pulse, thereby retaining all of the incorporated BrdU. In contrast, progenitor cells in the ventricular zone that have undergone multiple rounds of S and M phase following the pulse stain rather faintly due to dilution of the incorporated BrdU (Fig. 4c,d). This result indicates that greater numbers of neuronal cells in the *PS1*$^{-/-}$ brain exit the progenitor pool early to become postmitotic neurons, which is consistent with our results obtained with MAP2 immunostaining (Fig. 1). Furthermore, the BrdU-labelled neurons in the control telencephalon are localized appropriately within a well-defined cortical plate (Fig. 4c).

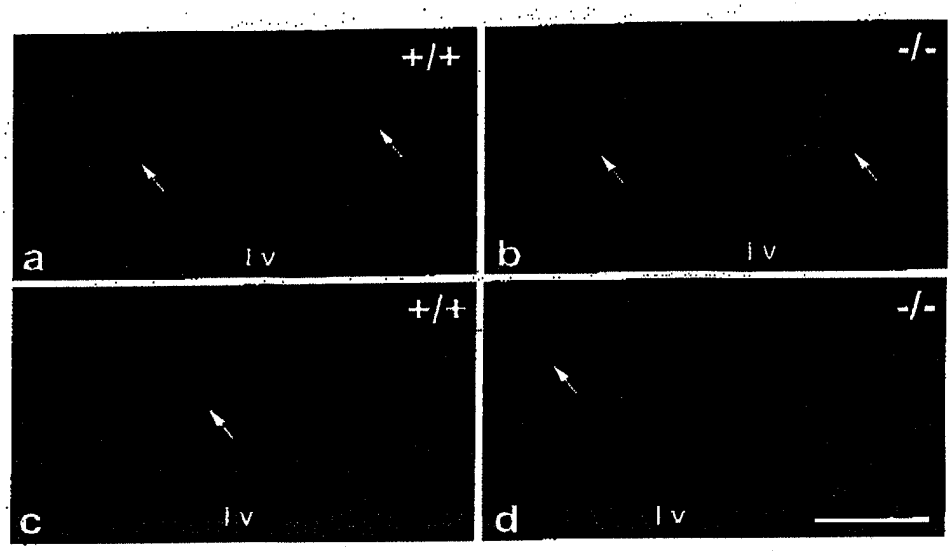

Fig. 3. Comparison of apoptosis in the *PS1*$^{-/-}$ and littermate control brains. Comparable transverse sections (7 μm) of *PS1*$^{-/-}$ and littermate control brains at E11.5 and E12.5 were processed for the TUNEL reaction and bisbenzimide staining. At E11.5 (a and b) and E12.5 (c and d), similar numbers of apoptotic cells were detected in the anterior telencephalon of the *PS1*$^{-/-}$ and littermate control brains. Arrows indicate TUNEL-positive apoptotic cells, which were also confirmed by their fragmented and/or condensed nuclei stained with bisbenzimide (not shown). lv, lateral ventricles. Bar, 100 μm.

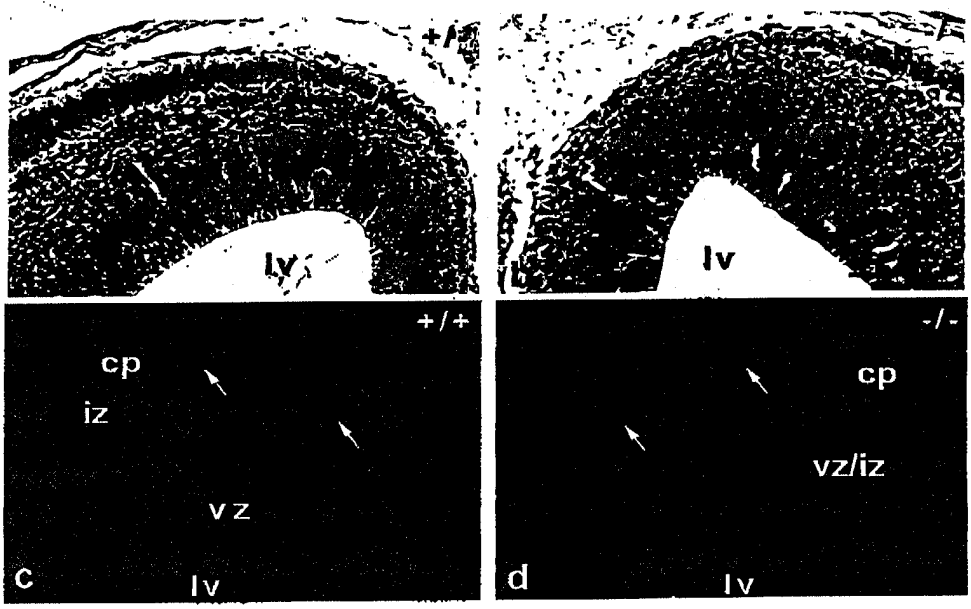

Fig. 4. Disrupted laminar organization of the cerebral hemisphere in *PS1*$^{-/-}$ mice. Comparable transverse sections (5 μm paraffin) of the *PS1*$^{-/-}$ and littermate control brains at E14.5 were stained with Hematoxylin and Eosin, and the anterior telencephalon of the *PS1*$^{-/-}$ and littermate control are shown in (a) and (b). The cortical plate (cp) is thinner and less well-defined in the *PS1*$^{-/-}$ brain (b) than in the control (a). The characteristic laminar organization is also disrupted in the *PS1*$^{-/-}$ brain (b), with an indistinct boundary between the ventricular (vz) and intermediate zones (iz). BrdU birthdating reveals the destination of newly generated neurons labelled at E10.5 when comparable transverse sections of the *PS1*$^{-/-}$ and littermate control brains are analyzed at E14.5 (c and d). Increased numbers of neurons in the cortical plate are labelled intensely by BrdU (arrows) in the *PS1*$^{-/-}$ brain (d). These intensely-stained neurons are distributed diffusely and are not organized into a well-defined cortical plate as in the control brain (c). Bar, 100 μm.

whereas the labelled neurons in the *PS1*$^{-/-}$ telencephalon are scattered diffusely across multiple cell layers (Fig. 4d), forming a disorganized cortical plate lacking a clear boundary with the adjacent intermediate and ventricular zones. These results support a role for PS1 in cortical layer formation and neuronal migration.

Molecular basis of premature neuronal differentiation in *PS1*$^{-/-}$ mice

To understand the mechanism underlying the premature neuronal differentiation observed in the *PS1*$^{-/-}$ brain, we examined the expression of genes in the Notch signalling pathway, which is known to be involved in cell-fate determination during neurogenesis in *Drosophila* (Artavanis-Tsakonas et al., 1999). The role of Notch receptors in murine neurogenesis is poorly understood. Mice lacking Notch1 or Notch2 function die at approximately E9 or E11, respectively, before cortical neurogenesis begins (Conlon et al., 1995; Hamada et al., 1999; Swiatek et al., 1994). An increased number of cells expressing proneural transcription factors, however, was identified in the midbrain and hindbrain of *Notch1*$^{-/-}$mice (de la Pompa et al., 1997). The basic helix-loop-helix transcription factors Hes1 and Hes5 (mammalian hairy and Enhancer-of-split homolog), which are downstream effectors of the Notch signalling pathway, have been shown to regulate murine neuronal differentiation (Ishibashi et al., 1995, 1994; Kageyama and Nakanishi, 1997; Ohtsuka et al., 1999; Tomita et al., 1996). We therefore first examined

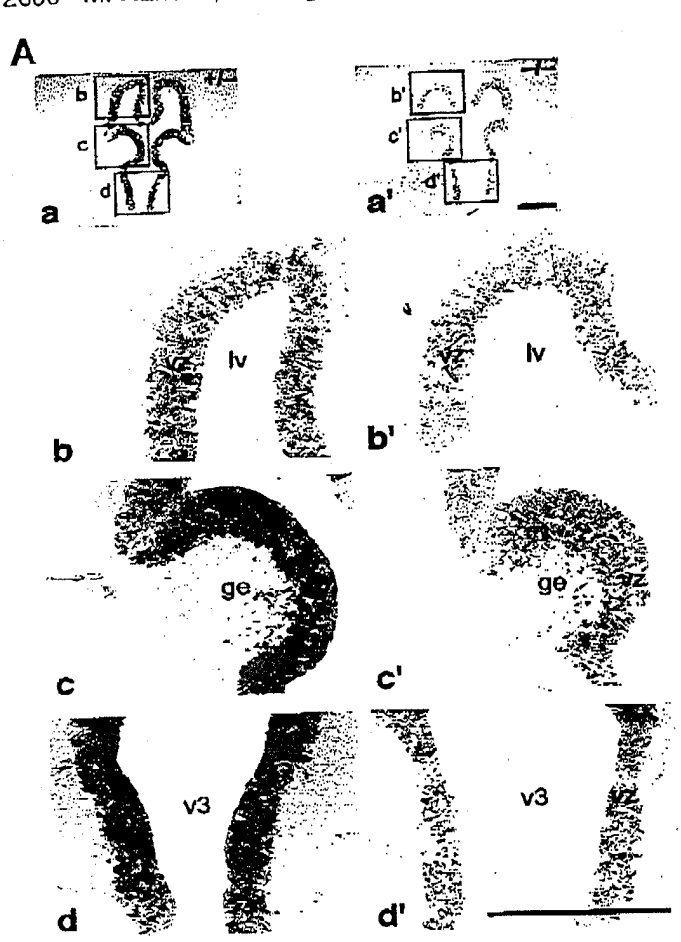

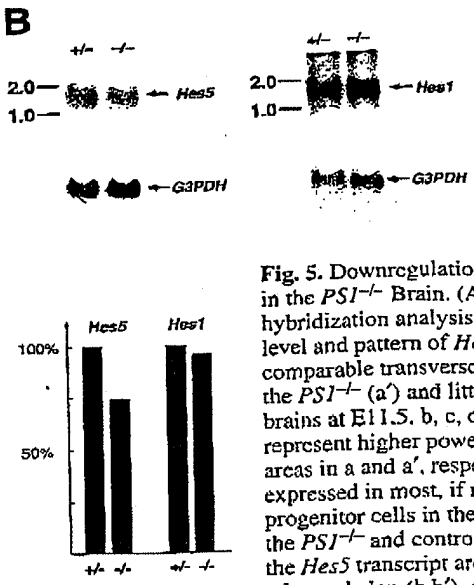

Fig. 5. Downregulation of *Hes5* expression in the *PS1*$^{-/-}$ Brain. (A) In situ hybridization analysis of the expression level and pattern of *Hes5* using comparable transverse sections (10 μm) of the *PS1*$^{-/-}$ (a′) and littermate control (a) brains at E11.5. b, c, d and b′, c′, d′ represent higher power views of the boxed areas in a and a′, respectively. *Hes5* is expressed in most, if not all, of the progenitor cells in the ventricular zone of the *PS1*$^{-/-}$ and control brains. The levels of the *Hes5* transcript are lower in the telencephalon (b,b′), ganglionic eminence (ge; c,c′) and diencephalon (d,d′) of the *PS1*$^{-/-}$ brain than in those of the control. *Hes5* expression is similarly reduced in the *PS1*$^{-/-}$ brain at E10.5 and E12.5 (data not shown). Abbreviations as in Fig. 1. Bar, 400 μm. (B) Northern analysis of *Hes5* and *Hes1* expression. Poly(A)$^+$ RNA (5 μg) was prepared from *PS1*$^{-/-}$ and littermate control (+/−) heads (n=8) at E11.5, and hybridized with *Hes5* or *Hes1* probes (Sasai et al., 1992; Takebayashi et al., 1995). The same blots were then hybridized with a control probe, *G3PDH*, to normalize the amounts of mRNA in each lane. The levels of *Hes5* and *Hes1* transcripts were quantified using NIH Image software, and the levels of these transcripts in the control are considered as 100%. A 25% and a 3% reduction in the levels of *Hes5* and *Hes1* transcripts were found in the *PS1*$^{-/-}$ brain, respectively.

expression of *Hes1* and *Hes5* transcripts by in situ hybridization and northern analyses to determine whether their expression patterns and levels are affected in *PS1*$^{-/-}$ mice.

In situ hybridization analysis of comparable sections of *PS1*$^{-/-}$ and littermate control brains at E11.5 showed that expression of *Hes5* is reduced in the *PS1*$^{-/-}$ brain (Fig. 5A). Consistent with previous studies (Akazawa et al., 1992), *Hes5* expression is localized to the ventricular zone within each brain region. In the control brain, the expression level of *Hes5* transcripts is higher in the ganglionic eminence (Fig. 5Ac) and diencephalon (Fig. 5Ad) than in the anterior telencephalon (Fig. 5Ab). In the *PS1*$^{-/-}$ brain, the expression level of *Hes5* is similar in the anterior telencephalon, ganglionic eminence and diencephalon, but is reduced relative to the control in each of these regions (Fig. 5Ab′,c′,d′). Therefore, the reduction in the level of *Hes5* transcripts is greater in the ganglionic eminence and diencephalon than in the anterior telencephalon. These regional differences in reduced *Hes5* expression parallel the regional differences in premature neuronal differentiation observed at the same developmental stage, with a more severe phenotype in the ganglionic eminence and diencephalon than in the anterior telencephalon of the *PS1*$^{-/-}$ brain. In addition, the region of *Hes5* expression is thinner, with fewer cell layers in the *PS1*$^{-/-}$ diencephalon (Fig. 5Ad′), corresponding to the thinned ventricular zone in this region of the *PS1*$^{-/-}$ brain (Fig. 1Bf,h).

Despite the precautions we took to perform in situ hybridization of *PS1*$^{-/-}$ and littermate control brain sections simultaneously and under identical conditions, it is still a less quantitative method than northern analysis for comparing the expression level of mRNA transcripts in *PS1*$^{-/-}$ and control mice. Therefore, we also performed northern analysis using poly(A)$^+$ RNA derived from the *PS1*$^{-/-}$ and littermate control heads at E11.5. The northern result showed an approximately 25% reduction in the level of the *Hes5* transcript in the *PS1*$^{-/-}$ brain, confirming the downregulation of *Hes5* expression in the absence of PS1 (Fig. 5B).

In situ hybridization analysis of *Hes1* expression revealed a similar pattern and level of expression in the *PS1*$^{-/-}$ and control brains at E11.5 (data not shown). Consistent with a previous report (Sasai et al., 1992), *Hes1* appears to be expressed in all cells of the embryonic brain with the highest expression in the progenitor cells of the ventricular zone. We also performed Northern analysis using poly(A)$^+$ RNA derived from the *PS1*$^{-/-}$ and littermate control heads at E11.5, and the result showed similar levels of *Hes1* transcripts in the *PS1*$^{-/-}$ and control brains, providing further confirmation

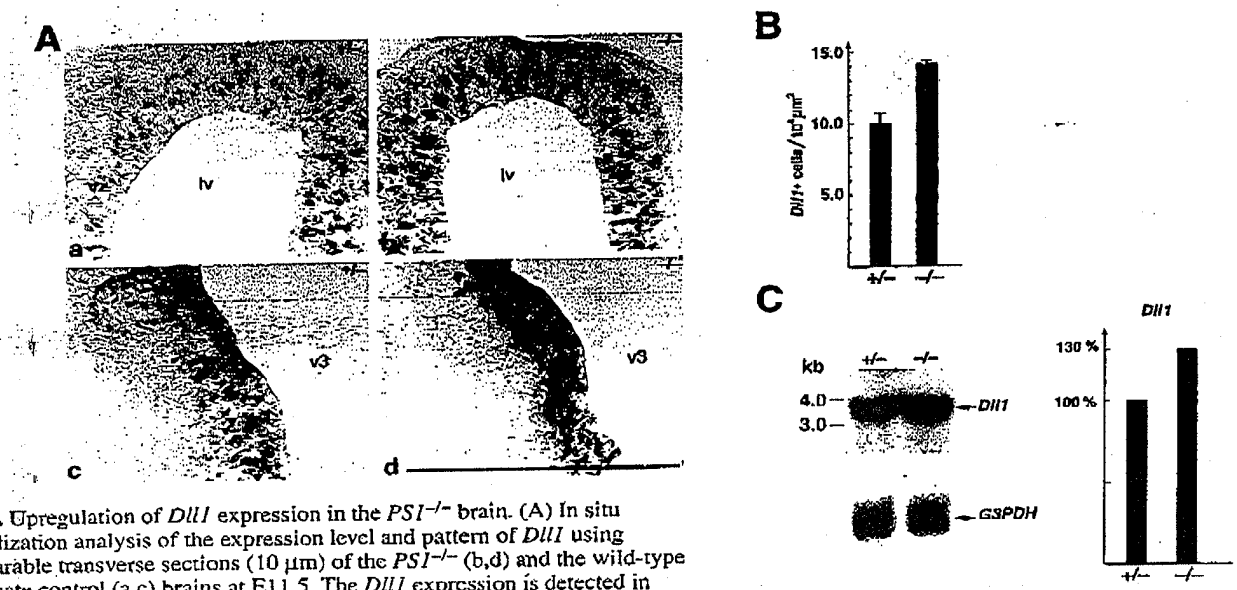

Fig. 6. Upregulation of *Dll1* expression in the *PS1*$^{-/-}$ brain. (A) In situ hybridization analysis of the expression level and pattern of *Dll1* using comparable transverse sections (10 µm) of the *PS1*$^{-/-}$ (b,d) and the wild-type littermate control (a,c) brains at E11.5. The *Dll1* expression is detected in scattered cells within the ventricular zone (vz). The levels of the *Dll1* transcript are higher in the telencephalon (a,b) and diencephalon (c,d) of the *PS1*$^{-/-}$ brain than in those of the control, and more *Dll1*-expressing cells are evident in the *PS1*$^{-/-}$ brain than in the control. Abbreviations as in Fig. 1. Bar, 400 µm. (B) Quantitative comparison of *Dll1*-expressing cells in the telencephalon of *PS1*$^{-/-}$ and littermate control brains at E11.5. The density of *Dll1*-expressing cells was determined by dividing the number of *Dll1*$^{+}$ cells by the area of half of the telencephalon. The data shown represent an average of one section from three brains per genotype. The density of *Dll1*-positive cells is increased by 40% in *PS1*$^{-/-}$ telencephalon. (C) Northern analysis of *Dll1* expression in the *PS1*$^{-/-}$ and control brains at E11.5. Total RNA (30 µg) was prepared from the heads of *PS1*$^{-/-}$ and littermate controls at E11.5, and hybridized with the *Dll1* probe (Bettenhausen et al., 1995). The same blot was then hybridized with a control probe, *G3PDH*, to normalize the amounts of mRNA in each lane. The levels of *Dll1* transcripts were quantified using NIH Image software, and a 30% increase in the level of *Dll1* transcripts was found in *PS1*$^{-/-}$ brains.

that expression of *Hes1* is unaffected in the *PS1*$^{-/-}$ brain (Fig. 5B).

In summary, the reduced expression of the Notch1 downstream target gene *Hes5* suggests a downregulation of Notch signalling in the absence of PS1. These results also provide a molecular basis for the premature neuronal differentiation observed in the *PS1*$^{-/-}$ brain, as suggested by the finding that neural progenitor cells prematurely differentiate into postmitotic neurons in *Hes5*$^{-/-}$ mice (Ohtsuka et al., 1999). The fact that expression of *Hes1* is unaltered in the *PS1*$^{-/-}$ mouse suggests that *Hes1* and *Hes5* expression might be regulated via different mechanisms.

It has been postulated in *Drosophila* that Notch and its ligand Delta are linked by a regulatory negative feedback loop under the transcriptional control of the *Enhancer-of-split* and *achaete-scute* complex gene products (Heitzler et al., 1996; Heitzler and Simpson, 1993, 1991). Expression of *Dll1*, which encodes a ligand of Notch1, is upregulated in the *Notch1*$^{-/-}$ mouse embryo (de la Pompa et al., 1997). We therefore examined expression of *Dll1* to determine whether it is upregulated in the *PS1*$^{-/-}$ brain. In situ hybridization analysis revealed that *Dll1* expression is confined to isolated cells in the ventricular zone, consistent with previous reports (Bettenhausen et al., 1995; Henrique et al., 1995). At E11.5, the number of *Dll1*-expressing cells is increased in the *PS1*$^{-/-}$ brain in all brain regions examined, including the anterior telencephalon (Fig. 6Aa,b) and diencephalon (Fig. 6Ac,d). Quantitative comparison of *Dll1*-expressing cells in the telencephalon revealed a 40% increase in the density of *Dll1*-expressing cells in the *PS1*$^{-/-}$ neuroepithelium (Fig. 6B). Northern analysis of total RNA derived from the *PS1*$^{-/-}$ and control heads at E11.5 showed a 30% increase in the level of *Dll1* transcripts in the *PS1*$^{-/-}$ brain relative to the control (Fig. 6C). These results indicate that lack of PS1 results in an increase in the number of *Dll1*-expressing cells and the overall expression level of *Dll1* transcripts, providing further evidence for the downregulation of Notch signalling.

To determine whether PS1 regulates Notch signalling at the level of transcription, translation and/or post-translational activation, we examined the *PS1*$^{-/-}$ and control brains for differences in the levels of *Notch1* expression and subcellular localization (Fig. 7). In situ hybridization analysis of comparable brain sections of the *PS1*$^{-/-}$ and littermate control at E11.5 revealed no significant differences in the expression pattern and the level of *Notch1* transcripts in the anterior telencephalon (Fig. 7Aa,b), ganglionic eminence (Fig. 7Ac,d) and diencephalon (Fig. 7Ae,f). Northern analysis confirmed that the level of the *Notch1* transcript is unaltered in the *PS1*$^{-/-}$ brain (Fig. 7B). Immunohistochemical analysis using a polyclonal antiserum (Logeat et al., 1998) raised against the ICD of mouse Notch1 showed intense Notch1 immunoreactivity in the ventricular zone, particularly in the ependymal cell layer and the adjacent progenitor cell layers (Fig. 7C). Notch1 immunoreactivity is localized predominantly to the cytoplasm and associated with the plasma membrane, although very low levels of nuclear Notch1 immunoreactivity could be detected in some progenitor cells (Fig. 7C). Comparison of corresponding sections of the *PS1*$^{-/-}$ and control brains revealed

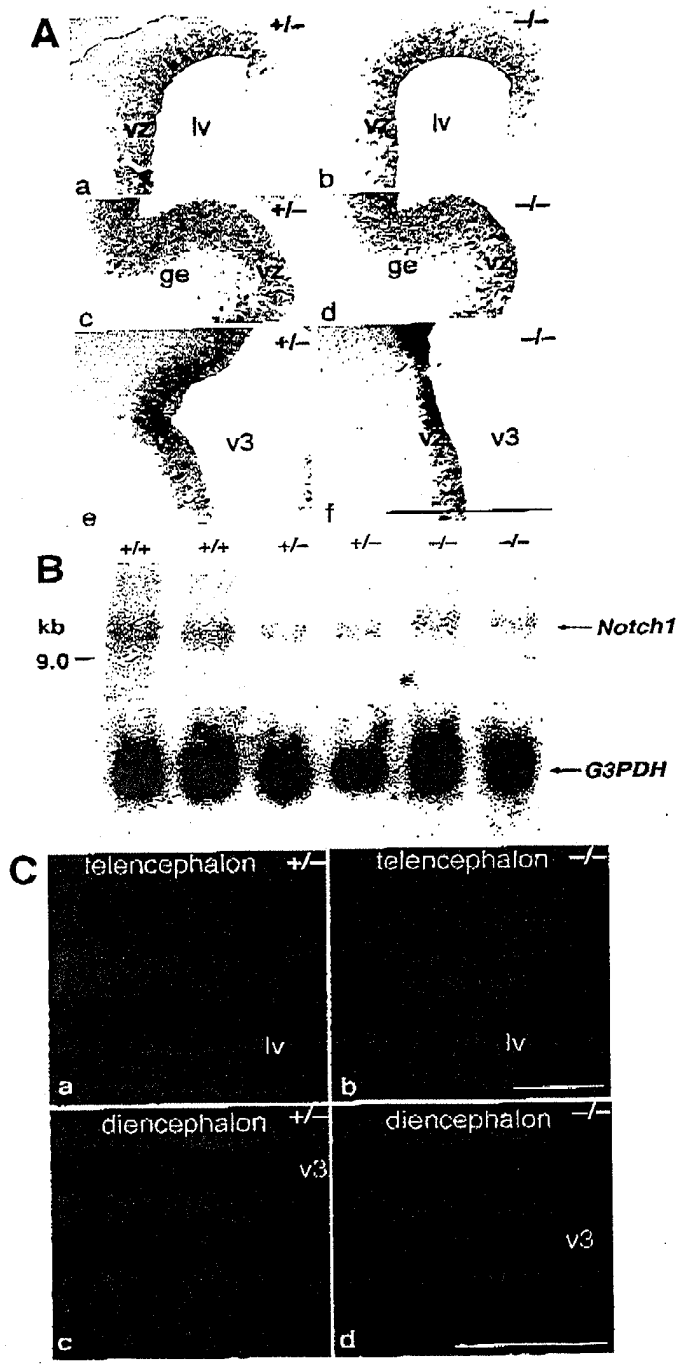

Fig. 7. Expression of *Notch1* in the *PS1–/–* and littermate control brains. (A) In situ hybridization analysis of the expression level and pattern of *Notch1* using comparable transverse sections (10 μm) of the $PS1^{-/-}$ (b,d,f) and littermate control (a,c,e) brains at E11.5. The levels of the *Notch1* transcript in the $PS1^{-/-}$ brain are similar to those of the control in the telencephalon (a,b), ganglionic eminence (c,d) and diencephalon (e,f). Abbreviations as in Fig. 1. (B) Northern analysis of *Notch1* expression. Total RNA was prepared from $PS1^{-/-}$ and littermate control (+/+,+/–) brains at E12.5, and hybridized with a 260 bp *Notch1* cDNA probe, which was generated by PCR amplification. The same blot was then hybridized with a control probe, *G3PDH*, to normalize the amounts of mRNA in each lane. Similar levels of *Notch1* transcripts are observed in $PS1^{-/-}$ and littermate control brains. (C) Confocal microscopic images of Notch1 immunostaining in the telencephalon (a,b) and diencephalon (c,d). Comparable transverse sections (10 μm) of the $PS1^{-/-}$ and littermate control brains at E11.5 were stained with a polyclonal antiserum raised against the mouse Notch1 ICD. The Notch1 immunoreactivity is similar in the $PS1^{-/-}$ and control brains, and is strongest in the ependymal cell layer and deep layers of the ventricular zone, with gradually weaker reactivity in the more superficial layers of the ventricular zone. The intense Notch1 immunostaining is localized to the cytoplasm and plasma membrane. Bars, 400 μm (A) and 50 μm (C).

no differences in the intensity of cytoplasmic and plasma membrane associated Notch1 immunoreactivity in the telencephalon and diencephalon (Fig. 7C). These results indicate that Notch signalling is unlikely to be regulated by PS1 at the levels of transcription and translation, thus most likely to be regulated at the level of post-translational activation. These findings are consistent with previous studies by us and other groups using cultured $PS1^{-/-}$ cells, which showed a requirement for PS1 in the normal production of NICD (De Strooper et al., 1999; Song et al., 1999).

Expression of *Notch1* and *Dll1* transcripts in the presomitic mesoderm of $PS1^{-/-}$ embryos

Previously, Wong et al. (1997) reported that expression of *Notch1* and *Dll1* transcripts is markedly reduced in the presomitic mesoderm of $PS1^{-/-}$ embryos. We observed increased *Dll1* expression and unchanged *Notch1* expression in the $PS1^{-/-}$ brain, however, raising the possibility that expression of *Notch1* and *Dll1* is regulated differently in the developing CNS and mesoderm. To address this issue, we examined the expression of *Notch1* and *Dll1* in the presomitic mesoderm in the $PS1^{-/-}$ and littermate control embryos by whole-mount in situ hybridization and northern analyses.

Whole-mount in situ hybridization analysis of $PS1^{-/-}$ and littermate control embryos at day 9.5 showed that *Notch1* and *Dll1* transcripts are expressed at highest levels in the presomitic mesoderm (Fig. 8A), consistent with previous reports (Bettenhausen et al., 1995; Franco Del Amo et al., 1992; Reaume et al., 1992). As we previously described (Shen et al., 1997), the somites in the caudal region of the $PS1^{-/-}$ embryo are disorganized and the boundaries between these somites are blurred (Fig. 8Ab,d). However, similar levels of *Notch1* and *Dll1* transcripts were detected in the presomitic mesoderm, which appears to be at its appropriate position (Fig. 8A). Because whole-mount in situ hybridization does not permit quantitative comparisons of mRNA expression levels, we carried out northern analysis to examine the levels of *Notch1* and *Dll1* transcripts. Northern analysis using total RNA derived from the tail buds of $PS1^{-/-}$ and control embryos at day 11.5, where *Notch1* and *Dll1* are expressed at their highest level, revealed similar levels of *Notch1* transcripts and increased levels of *Dll1* transcripts in the $PS1^{-/-}$ embryo relative to the control (Fig. 8B). These results indicate that regulation of Notch signalling does not differ in the CNS and paraxial mesoderm.

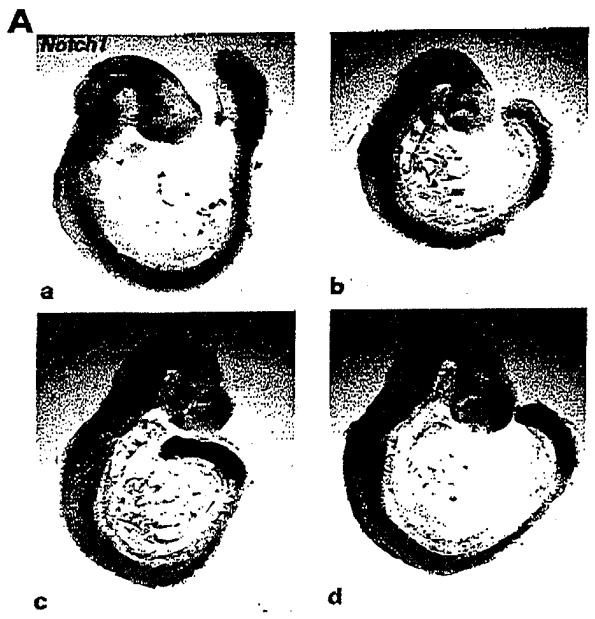

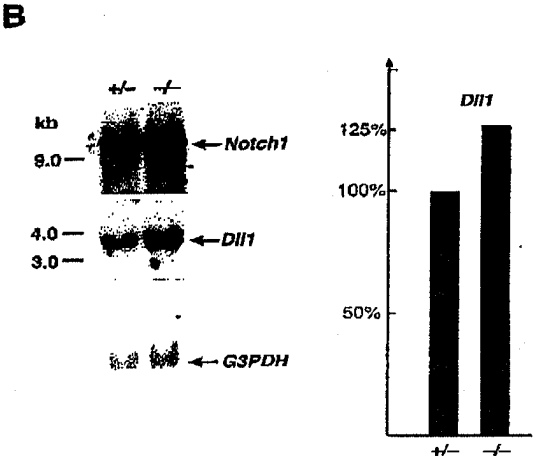

Fig. 8. Expression of *Notch1* and *Dll1* in the presomitic mesoderm of $PS1^{-/-}$ embryos. (A) Whole-mount in situ hybridization analysis of *Dll1* and *Notch1* expressions at E9.5. *Notch1* is strongly expressed in the presomitic mesoderm, with lower levels of expression in the dorsal spinal cord and hindbrain (a,b). *Dll1* is also intensely expressed in the presomitic mesoderm, with lower levels of expression throughout the CNS and in the posterior portion of somites (c,d). The levels of *Notch1* and *Dll1* transcripts in the presomitic mesoderm of $PS1^{-/-}$ embryos are comparable to those of the control (a-d). (B) Northern analysis of *Dll1* and *Notch1* expression. Total RNA (30 μg) was prepared from eight tail buds per genotype at E11.5, and hybridized first with the *Dll1* probe then with the *Notch1* probe. The same blot was then hybridized with a control probe, *G3PDH*, to normalize the amounts of mRNA in each lane. The level of *Dll1* transcripts is upregulated in the $PS1^{-/-}$ embryos, while the level of *Notch1* transcripts is similar to the control.

DISCUSSION

Our previous characterization of $PS1^{-/-}$ mice documented specific defects in central nervous system development, revealing a function for PS1 in the mammalian brain (Shen et al., 1997). Here we characterize the mechanisms underlying the progressive reduction in neural progenitor cells that we observed in the $PS1^{-/-}$ brain, as depicted schematically in Fig. 9. Analysis of the $PS1^{-/-}$ brain between E10.5 and 13.5 revealed increased numbers of postmitotic neurons detected by MAP2 (Fig. 1) and TuJ1 (data not shown) immunoreactivity in the telencephalon and diencephanlon. The premature neuronal differentiation in the $PS1^{-/-}$ brain leads to a reduction in the neural progenitor population and thinning of the ventricular zone. This is particularly evident in the diencephalon, where increased MAP2 immunoreactivity at E10.5 (Fig. 1Ab) is followed by decreased BrdU immunoreactivity at E11.5 (Fig. 2Bf). These results demonstrate that lack of PS1 function leads to an increase in the number of differentiated postmitotic neurons at the expense of progenitor cells during early neurogenesis, resulting in a partial depletion of the neural progenitor population. These observations provide an explanation for the progressive reduction of the neural progenitor population and the subsequent reduction of neuronal population previously observed in the $PS1^{-/-}$ brain (Shen et al., 1997). Taken together, these findings support a novel role for PS1 in the regulation of neuronal differentiation and a cell-fate decision between neural progenitor cells and postmitotic neurons in the developing brain.

We further investigated the role of PS1 in neuronal proliferation, survival and migration during early neural development. The similar proliferation rates of neural progenitor cells in the $PS1^{-/-}$ and control brains, as measured by the percentage of BrdU-labelled cells to total progenitor cells, suggest that PS1 is not involved in the regulation of neural progenitor proliferation (Fig. 2 and Table 1). Our analysis of the $PS1^{-/-}$ brain at E11.5 and 12.5 also shows that lack of PS1 does not result in increased apoptotic cell death at these early neural developmental stages (Fig. 3 and Table 2). Severe neuronal loss was, however, observed in specific regions of the $PS1^{-/-}$ telencephalon beginning at E16.5 (Shen et al., 1997). Thus, it remains possible that PS1 influences neuronal survival during later stages of neurogenesis.

An involvement of wild-type and FAD-linked mutant presenilins in regulation of apoptosis has been suggested by previous investigations in various cell culture systems (Deng et al., 1996; Guo et al., 1996; Kim et al., 1997; Loetscher et al., 1997; Roperch et al., 1998; Vito et al., 1996; Wolozin et al., 1996; Zhang et al., 1998). The Notch signalling pathway has also been implicated in the regulation of apoptosis, with Notch activity appearing to promote cell survival. Loss of Notch activity in *Drosophila* is spatiotemporally correlated with increased levels of apoptosis (Kim et al., 1996; Van Doren et al., 1992). In mice lacking *Notch2* function, increased apoptosis was observed in neural tissues (Hamada et al., 1999). Finally, a connection between Presenilin and Notch activity in apoptosis was suggested by the finding that mutant flies either overexpressing or lacking PS exhibited increased levels of apoptotic cell death; this phenotype was suppressed in both cases by expression of constitutively active Notch (Ye and Fortini, 1999). It is not yet clear whether the loss of neural progenitor cells and neurons observed in the $PS1^{-/-}$ brain is

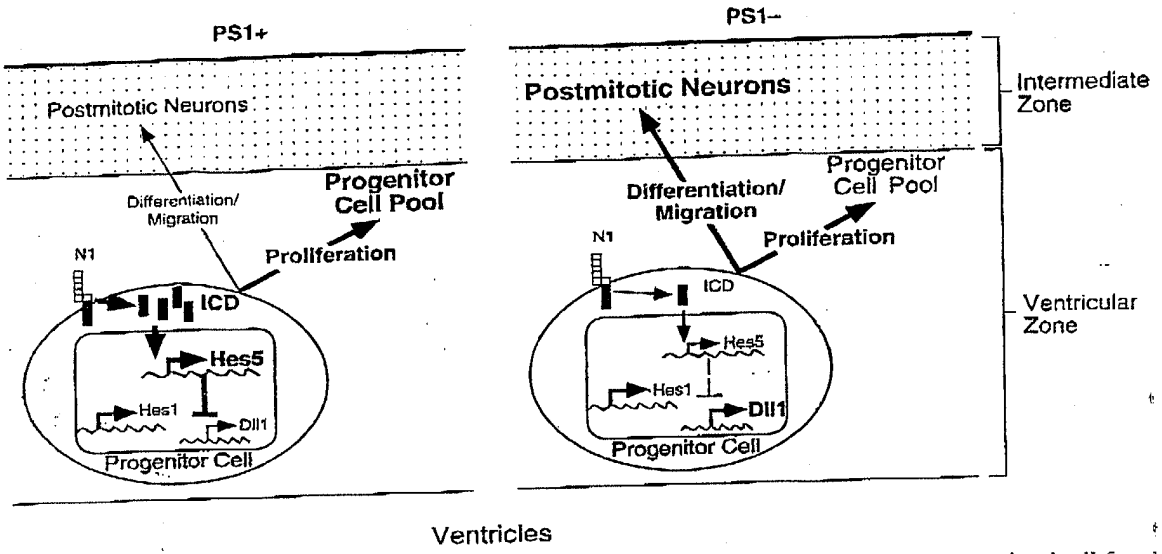

Fig. 9. Role of PS1 in neural development and the Notch signalling pathway. The Notch signalling events and associated cell-fate decisions of neural progenitor cells during early neurogenesis are depicted schematically in the presence (PS1+, left) and absence (PS1–, right) of PS1. Thick arrows and bold type represent relative increases. In the presence of PS1, the proliferation of neural progenitor cells is favored by activation of the Notch signalling pathway. A small proportion of neural progenitor cells residing in the ventricular zone gives rise to postmitotic neurons, which migrate superficially to the intermediate zone, while the remainder produce a steady expansion in the progenitor pool through continued proliferation. In the absence of PS1, Notch signalling activity is diminished, leading to decreased levels of nuclear Notch ICD, reduced *Hes5* expression and increased *Dll1* expression. This reduced Notch signalling alters the cell-fate decision of neural progenitor cells in favor of the generation of postmitotic neurons, resulting in a relative reduction in the neural progenitor pool despite a normal proliferation rate. Although total numbers of postmitotic neurons in the absence of PS1 are increased early in neurogenesis, the reduced neural progenitor pool leads to a reduction in the overall numbers of postmitotic neurons in the cortical plate at later stages.

cell-autonomous, and whether downregulation of the Notch1 signalling activity plays a direct role. We are currently investigating the mechanism underlying this region-specific neuronal loss by generating conditional $PS1^{-/-}$ mice lacking PS1 function specifically in neuronal cell types.

The results of our neuroanatomical and BrdU birthdating analysis support a role for PS1 in the regulation of neuronal migration during cortical neurogenesis. Examination of the $PS1^{-/-}$ brain stained with Hematoxylin and Eosin suggested disruption of the normal architecture of the developing forebrain, with an indistinct boundary between the ventricular and intermediate zones and thinning of the cortical plate (Fig. 4). The BrdU birthdating study revealed disorganization of postmitotic neurons in the developing cortical plate (Fig. 4). However, our birthdating analysis was limited to $PS1^{-/-}$ brains at E14.5, due to severe cerebral hemorrhage often associated with $PS1^{-/-}$ brains at later developmental stages. Therefore, whether cortical lamination defects in the $PS1^{-/-}$ brain are similar to those seen in the reeler mouse is unclear. Extensive BrdU birthdating analysis on *PS1* conditional knockout mice, in which PS1 inactivation is restricted to the neuronal population, should address this question. The mechanism by which PS1 regulates cortical layer formation and neuronal migration is unknown. The perturbed laminar organization may be associated with the progressive loss of Cajal-Retzius neurons observed in the $PS1^{-/-}$ brain; however, the cause of the progressive loss of these neurons is unclear. It is also possible that PS1 is an upstream regulator or a downstream target of Cdk5/p35 or mDab1, both of which play an important role in neuronal migration (Chae et al., 1997; Howell et al., 1997; Ohshima et al., 1996). Reduced Notch signalling in $PS1^{-/-}$ mice may also contribute to the neuronal migration defects, as suggested by the findings in *Drosophila* that Notch genetically interacts with Abl and its intracellular domain binds directly to Dab in vitro (Giniger, 1988).

To understand the mechanism by which PS1 controls neuronal differentiation during neurogenesis, we examined the expression of genes involved in the Notch signalling pathway: *Notch1*, *Dll1* and the Notch downstream effector genes *Hes1* and *Hes5*. Previous studies have suggested a connection between Notch signalling and the regulation of neuronal differentiation. Premature neuronal differentiation has been observed at E10.5 in mutant mice lacking Hes1, Hes5, or both Hes1 and Hes5 (Ishibashi et al., 1995; Ohtsuka et al., 1999). Continuous overexpression of *Hes1* by retroviral infection inhibits neuronal differentiation (Ishibashi et al., 1994). Here we have shown that expression of *Hes5* transcripts is downregulated in the $PS1^{-/-}$ brain, particularly in the ganglionic eminence and diencephalon, whereas expression of *Hes1* is unaffected (Fig. 5). These results suggest that Notch signalling is compromised in the absence of PS1, as evidenced by the downregulation of *Hes5* expression. In addition, regulation of Notch downstream target genes appears to be complex, since PS1 regulates specifically the expression of *Hes5* but not *Hes1*. It is not yet clear whether Hes5 is the only downstream target of PS1 in the regulation of neuronal differentiation during neurogenesis. The extent of the premature differentiation of neural progenitor cells observed in the $PS1^{-/-}$ and $Hes5^{-/-}$

brains at E10.5 appears to be similar (Fig. 1; Ohtsuka et al., 1999). Examination of the *PS1*$^{-/-}$ and *Hes5*$^{-/-}$ brains at later embryonic stages for differences in neuronal differentiation and neurogenesis might reveal whether PS1 controls neuronal differentiation and cell fate decision between progenitor cells and postmitotic neurons through the regulation of *Hes5*.

Further supporting evidence for the downregulation of Notch signalling includes the upregulation of *Dll1* expression in *PS1*$^{-/-}$ mice. Our results demonstrated that the level of *Dll1* transcripts is elevated in the brain and the presomitic mesoderm of *PS1*$^{-/-}$ mice and more *Dll1*-expressing cells are present in the *PS1*$^{-/-}$ brain (Figs 6, 8). Studies in *Xenopus* and the chick embryo have shown that *Dll1* homologues are expressed in the prospective neurons and their expression precedes expression of early neuronal markers (Chitnis et al., 1995; Henrique et al., 1995). An increase in *Dll1*-expressing cells is consistent with the presence of more differentiated neurons identified in the *PS1*$^{-/-}$ brain.

Lack of PS1 function was previously reported to result in reduced transcription of *Notch1* and *Dll1* in the presomitic mesoderm of the *PS1*$^{-/-}$ embryo, suggesting a role for PS1 in the regulation of *Notch1* and *Dll1* at the transcriptional level (Wong et al., 1997). We detected unaltered levels of *Notch1* transcripts (Figs 7, 8) and elevated levels of *Dll1* transcripts (Figs 6, 8) both in the *PS1*$^{-/-}$ embryonic brain and presomitic mesoderm. Furthermore, we observed no differences in the intensity of cytoplasmic and plasma membrane associated Notch1 immunoreactivity in the *PS1*$^{-/-}$ and control brains (Fig. 7). Therefore, PS1 is unlikely to be involved in the regulation of Notch1 transcription and translation in the developing mammalian brain and paraxial mesoderm. However, PS1 is involved in the activation of Notch signalling, as indicated by the alterations of *Hes5* and *Dll1* expression in *PS1*$^{-/-}$ mice (Figs 5, 6, 8). These results are consistent with recent studies showing that similar levels of furin-cleaved Notch1 fragment were detected in the *PS1*$^{-/-}$ and control mouse brains by immunoprecipitation-western analysis (De Strooper et al., 1999). Analysis of the proteolytic processing of truncated Notch1 proteins in cultured cells derived from *PS1*$^{-/-}$ mice has shown that PS1 is required for efficient release of the Notch1 ICD (De Strooper et al., 1999; Song et al., 1999). The present study supports such a role for PS1 in the regulation of Notch signalling, and further provides evidence that the reduced Notch processing observed in *PS1*$^{-/-}$ cells is functionally significant in neural development.

Finally, our results indicate an important difference in the consequences of reduced Notch signalling during neurogenesis in *Drosophila* and mice. In *Drosophila* neurogenesis, Notch controls a cell-fate decision between two cell types produced from a multipotent common precursor, promoting epidermal production at the expense of neuronal production. Loss of function mutations in Notch thereby lead to excessive neuronal production (Artavanis-Tsakonas et al., 1999). Our findings suggest that Notch1 regulates a cell-fate choice between neural progenitor cells and differentiated neurons early in murine neurogenesis, promoting regeneration of neuronal precursor cells at the expense of differentiation of postmitotic neurons. Therefore, although Notch functions to suppress the production of postmitotic neurons in both mice and *Drosophila*, downregulation of Notch activity in mice and *Drosophila* results in a reduction in neuronal population and a neurogenic phenotype, respectively.

In summary, we demonstrate that lack of PS1 during neural development results in a reduction in Notch signalling activity, as indicated by reduced *Hes5* expression and increased *Dll1* expression, which alters the cell-fate decision of neural progenitor cells in favor of differentiation into postmitotic neurons (Fig. 9). The roles of PS1 and the Notch signalling pathway in the adult brain are currently unknown. A recent report documented the existence of Notch1-expressing neural stem cells residing in the ependymal cell layer of the adult rat brain (Johansson et al., 1999), which suggests that Notch signalling may be involved in the maintenance of a neural stem cell population in the adult brain. Understanding the roles of PS1 and Notch signalling in the adult brain may therefore lead to novel therapeutic strategies for combating the neuronal and synaptic loss that occurs in neurodegenerative illnesses such as Alzheimer's disease.

We thank Drs Spyros Artavanis-Tsakonas, Bruce Yankner, Dennis Selkoe, Ken Kosik, Chris Walsh, Rudy Tanzi and anonymous reviewers for comments on the manuscript; Drs Ryoichiro Kageyama, Gerry Weinmaster and Randy Johnson, for plasmids; Dr Alain Israel for Notch1 antiserum; and Dr Ken Kosik for the anti-MAP2 antibody. We are grateful to Ricardo Soto and Huakui Yu for their excellent technical assistance. This research was supported in part by the American Federation for Aging Research, the Alzheimer's Association and NINDS.

REFERENCES

Akazawa, C., Sasai, Y., Nakanishi, S. and Kageyama, R. (1992). Molecular characterization of a rat negative regulator with a basic helix-loop-helix structure predominantly expressed in the developing nervous system. *J. Biol. Chem.* **267**, 21879-21885.

Artavanis-Tsakonas, S., Rand, M. D. and Lake, R. J. (1999). Notch signaling: cell fate control and signal integration in development. *Science* **284**, 770-776.

Baumeister, R., Leimer, U., Zweckbronner, I., Jakubek, C., Grunberg, J. and Haass, C. (1997). Human presenilin-1, but not familial Alzheimer's disease (FAD) mutants, facilitate *Caenorhabditis elegans* Notch signalling independently of proteolytic processing. *Genes Funct.* **2**, 149-159.

Bettenhausen, B., de Angelis, M., Simon, D., Guenet, J. and Gossler, A. (1995). Transient and restricted expression during mouse embryogenesis of Dll1, a murine gene closely related to *Drosophila* Delta. *Development* **121**, 2407-2418.

Chae, T., Kwon, Y., Bronson, R., Dikkes, P., Li, E. and Tsai, L.-H. (1997). Mice lacking p35, a neuronal specific activator of cdk5, display cortical lamination defects, seizures, and adult lethality. *Neuron* **18**, 29-42.

Chitnis, A., Henrique, D., Lewis, J., Ish-Horowicz, D. and Kintner, C. (1995). Primary neurogenesis in *Xenopus* embryos regulated by a homologue of the *Drosophila* neurogenic gene *Delta*. *Nature* **375**, 761-766.

Conlon, R. A., Reaume, A. G. and Rossant, J. (1995). Notch 1 is required for the coordinate segmentation of somites. *Development* **121**, 1533-1545.

Crandall, J. E., Jacobson, M. and Kosik, K. S. (1986). Ontogenesis of microtubule-associated protein 2 (MAP2) in embryonic mouse cortex. *Brain Res.* **393**, 127-133.

de la Pompa, J. L., Wakeham, A., Correia, K. M., Samper, E., Brown, S., Aguilera, R. J., Nakano, T., Honjo, T., Mak, T. W., Rossant, J. and Conlon, R. A. (1997). Conservation of the Notch signalling pathway in mammalian neurogenesis. *Development* **124**, 1139-1148.

De Strooper, B., Annaert, W., Cupers, P., Saftig, P., Craessaerts, K., Mumm, J. S., Schroeter, E. H., Schrijvers, V., Wolfe, M. S., Ray, W. J., Goate, A. and Kopan, R. (1999). A presenilin-1-dependent gamma-secretase-like protease mediates release of Notch intracellular domain [see comments]. *Nature* **398**, 518-522.

Deckwerth, T. and Johnson, E. (1993). Temporal analysis of events associated with programmed cell death (apoptosis) of sympathetic neurons deprived of nerve growth factor. *J. Cell Biol.* **123**, 1207-22.

Deng, G., Pike, C. J. and Cotman, C. W. (1996). Alzheimer-associated presenilin-2 confers increased sensitivity to apoptosis in PC12 cells. *FEBS Lett.* **39979**, 50-54.

Franco Del Amo, F., Smith, D., Swiatek, P., Gendron-maguire, M.,

Greenspan, R., McMahon, A. and Gridley, T. (1992). Expression pattern of Motch, a mouse homolog of *Drosophila Notch*, suggests an important role in early postimplantation mouse development. *Development* **115**, 737-744.

Gavrieli, Y., Sherman, Y. and Ben-Sasson, S. (1992). Identification of programmed cell death in situ via specific labelling of nuclear DNA fragmentation. *J. Cell Biol.* **119**, 493-501.

Giniger, E. (1988). A role for Abl in Notch signalling. *Neuron* **20**, 667-81.

Gratzner, H. G. (1982). Monoclonal antibody to 5-bromo- and 5-iododeoxyuridine: A new reagent for detection of DNA replication. *Science* **218**, 474-475.

Guo, Q., Furukawa, K., Sopher, B., Pham, D., Xie, J., Robinson, N., Nartin, G. and Mattson, M. (1996). Alzheimer's PS1 mutation perturbs calcium homeostasis and sensitizes PC-12 cells to death induced by amyloid β-peptide. *Neurorep.* **8**, 379-383.

Hamada, Y., Kadokawa, Y., Okabe, M., Ikawa, M., Coleman, J. and Tsujimoto, Y. (1999). Mutation in ankyrin repeats of the mouse *Notch2* gene induces early embryonic lethality. *Development* **126**, 3415-3424.

Hartmann, D., De Strooper, B. and Saftig, P. (1999). Presenilin-1 deficiency leads to loss of Cajal-Retzius neurons and cortical dysplasia similar to human type 2 lissencephaly. *Curr. Biol.* **9**, 719-727.

Heitzler, P., Bourouis, M., Ruel, L., Carteret, C. and Simpson, P. (1996). Genes of the Enhancer of split and achaete-scute complexes are required for a regulatory loop between Notch and Delta during lateral signalling in *Drosophila*. *Development* **122**, 161-171.

Heitzler, P. and Simpson, P. (1993). Altered epidermal growth factor-like sequences provide evidence for a role of *Notch* as a receptor in cell fate decisions. *Development* **117**, 1113-1123.

Heitzler, P. and Simpson, P. (1991). The choice of cell fate in the epidermis of *Drosophila*. *Cell* **64**, 1083-1092.

Henrique, D., Adam, J., Myat, A., Chitnis, A., Lewis, J. and Ish-Horowicz, D. (1995). Expression of a Delta homologue in prospective neurons in the chick. *Nature* **375**, 787-790.

Hogan, B., Beddington, R., Constantini, F. and Lacy, E. (1994). *Manipulating The Mouse Embryo: A Laboratory Manual*, 2nd Edition. Cold Spring Harbor Laboratory Press, NY.

Howell, B., Hawkes, R., Soriano, P. and Cooper, J. (1997). Neuronal position in the developing brain is regulated by mouse *disabled-1*. *Nature* **389**, 733-737.

Ishibashi, M., Ang, S. L., Shiota, K., Nakanishi, S., Kageyama, R. and Guillemot, F. (1995). Targeted disruption of mammalian hairy and Enhancer of split homolog-1 (HES-1) leads to up-regulation of neural helix-loop-helix factors, premature neurogenesis, and severe neural tube defects. *Genes Dev.* **9**, 3136-1348.

Ishibashi, M., Moriyoshi, K., Sasai, Y., Shiota, K., Nakanishi, S. and Kageyama, R. (1994). Persistent expression of helix-loop-helix factor HES-1 prevents mammalian neural differentiation in the central nervous system. *EMBO J.* **13**, 1799-1805.

Johansson, C. B., Momma, S., Clarke, K. L., Risling, M., Lendahl, U. and Frisen, J. (1999). Identification of a neural stem cell in the adult mammalian central nervous system. *Cell* **96**, 25-34.

Kageyama, R. and Nakanishi, S. (1997). Helix-loop-helix factors in growth and differentiation of the vertebrate nervous system. *Curr. Opin. Genet. Dev.* **7**, 659-665.

Kim, J., Sebring, A., Esch, J., Kraus, M., Vorwerk, K., Magee, J. and Carroll, S. (1996). Integration of positional signals and regulation of wing formation and identity by *Drosophila vestigial* gene. *Nature* **382**, 133-138.

Kim, T., Pettingell, W., Jung, Y., Kovacs, D. and Tanzi, R. (1997). Alternative cleavage of Alzheimer-associated presenilins during apoptosis by a Caspase-3 family protease. *Science* **277**, 373-376.

Levitan, D., Doyle, T. G., Brousseau, D., Lee, M. K., Thinakaran, G., Slunt, H. H., Sisodia, S. S. and Greenwald, I. (1996). Assessment of normal and mutant human presenilin function in *Caenorhabditis elegans*. *Proc. Natl. Acad. Sci. USA* **93**, 14940-14944.

Levitan, D. and Greenwald, I. (1998). Effects of SEL-12 presenilin on LIN-12 localization and function in *Caenorhabditis elegans*. *Development* **125**, 3599-3506.

Levitan, D. and Greenwald, I. (1995). Facilitation of *lin-12*-mediated signalling by *sel-12*, a *Caenorhabditis elegans S182* Alzheimer's disease gene. *Nature* **377**, 351-354.

Loetscher, H., Deuschle, U., Brockhaus, M., Reinhardt, D., Nelboeck, P., Mous, J., Grunberg, J., Haass, C. and Jacobsen, H. (1997). Presenilins are processed by caspase-type proteases. *J. Biol. Chem.* **272**, 20655-20659.

Logeat, F., Bessia, C., Brou, C., LeBail, O., Jarriault, S., Seldah, N. and Israel, A. (1998). The Notch1 receptor is cleaved constitutively by a furin-like convertase. *Proc. Natl. Acad. Sci. USA* **95**, 8108.

McConnell, S. K. (1995). Constructing the cerebral cortex: neurogenesis and fate determination. *Neuron* **15**, 761-768.

Ohshima, T., Ward, J., Huh, C.-G., Longenecker, G., Veeranna, Pant, H., Brady, R., Martin, L. and Kulkarni, A. (1996). Targeted disruption of the cyclin-dependent kinase 5 gene results in abnormal corticogenesis, neuronal pathology and perinatal death. *Proc. Natl. Acad. Sci. USA* **93**, 11173-11178.

Ohtsuka, T., Ishibashi, M., Gradwohl, G., Nakanishi, S., Guillemot, F. and Kageyama, R. (1999). Hes1 and Hes5 as notch effectors in mammalian neuronal differentiation. *EMBO J.* **18**, 2196-2207.

Reaume, A., Conlon, R., Zirngibl, R., Yamaguchi, T. and Rossant, J. (1992). Expression analysis of a Notch homologue in the mouse embryo. *Dev. Biol.* **154**, 377-387.

Roperch, J. P., Alvaro, V., Prieur, S., Tuynder, M., Nemani, M., Lethrosne, F., Piouffre, L., Gendron, M. C., Israeli, D., Dausset, J., Oren, M., Amson, R. and Telerman, A. (1998). Inhibition of presenilin 1 expression is promoted by p53 and p21WAF-1 and results in apoptosis and tumor suppression (In Process Citation). *Nat. Med.* **4**, 835-838.

Sasai, Y., Kageyama, R., Tagawa, Y., Shigemoto, R. and Nakanishi, S. (1992). Two mammalian helix-loop-helix factors structurally related to *Drosophila hairy* and *Enhancer of split*. *Genes Dev.* **6**, 2620-2634.

Schaeren-Wiemers, N. and Gerfin-Moser, A. (1993). A single protocol to detect transcripts of various types and expression levels in neural tissue and cultured cells: in situ hybridization using digoxigenin-labelled cRNA probes. *Histochemistry* **100**, 431-440.

Selkoe, D. J. (1998). The cell biology of β-amyloid precursor protein and presenilin in Alzheimer's disease. *Trends Cell Biol.* **8**, 447-453.

Shen, J., Bronson, R. T., F, C. D., Xia, W., Selkoe, D. J. and Tonegawa, S. (1997). Skeletal and CNS defects in presnilin-1 deficient mice. *Cell* **89**, 629-639.

Song, W., Nadeau, P., Yuan, M., Yang, X., Shen, J. and Yankner, B. A. (1999). Proteolytic release and nuclear translocation of notch-1 are induced by presenilin-1 and impaired by pathogenic presenilin-1 mutations. *Proc. Natl. Acad. Sci. USA* **96**, 6959-6963.

Struhl, G. and Greenwald, I. (1999). Presenilin is required for activity and nuclear access of Notch in Drosophila [see comments]. *Nature* **398**, 522-525.

Swiatek, P. J., Lindsell, C. E., Franco del Amo, F., Weinmaster, G. and Gridley, T. (1994). Notch 1 is essential for postimplantation development in mice. *Genes Dev.* **8**, 707-719.

Takahashi, T., Nowakowski, R. S. and Caviness, V. S., Jr. (1995). The cell cycle of the pseudostratified ventricular epithelium of the embryonic murine cerebral wall. *J. Neurosci.* **15**, 6046-6057.

Takebayashi, K., Akazawa, C., Nakanishi, S. and Kageyama, R. (1995). Structure and promoter analysis of the gene encoding the mouse helix-loop-helix factor HES-5. Identification of the neural precursor cell-specific promoter element. *J. Biol. Chem.* **270**, 1342-1349.

Tomita, K., Ishibashi, M., Nakahara, K., Ang, S., Nakanishi, S. and Kageyama, R. (1996). Mammalian *hairy* and *Enhancer of split* homolog 1 regulates differentiation of retinal neurons and is essential for eye morphogenesis. *Neuron* **16**, 723-734.

Van Doren, M., Powell, P. A., Pasternak, D., Singson, A. and Posakony, J. W. (1992). Spatial regulation of proneural gene activity: auto- and cross-activation of *achaete* is antagonized by *extramacrochaetae*. *Genes Dev.* **6**, 2592-2605.

Vito, P., Lacana, E. and D'Adamio, L. (1996). Interfering with apoptosis:Ca^{2+} Binding protein ALG-2 and Alzhermer's disease gene ALG-3. *Science* **271**, 521-525.

Wolozin, B., Iwasaki, K., Vito, P., Ganjei, K., Lacana, E., Sunderland, T., Zhao, B., W, K. J., Wasco, W. and D'Adamio, L. (1996). PS2 participates in cellular apoptosis: Constitutive activity conferred by Alzheimer mutation. *Science* **274**, 1710-1713.

Wong, P., Zhen, H., Chen, H., Becher, M. W., Sirinathsinghji, D. J., Trumbauer, M. E., Proce, D. L., Van der Ploeg, L. H. T. and Sisodia, S. S. (1997). Presenilin 1 is required for Notch 1 and D111 expression in the paraxial mesoderm. *Nature* **397**, 288.

Ye, Y. and Fortini, M. (1999). Apoptotic activities of wild-type and Alzheimer's disease-related mutant presenilins in *Drosophila melangaster*. *J. Cell Biol.* **146**, 1351-1364.

Ye, Y., Lukinova, N. and Fortini, M. E. (1999). Neurogenic phenotypes and altered Notch processing in Drosophila Presenilin mutants. *Nature* **398**, 525-529.

Zhang, Z., Hartmann, H., Do, V. M., Abramowski, D., Sturchler-Pierrat, C., Staufenbiel, M., Sommer, B., va de Wetering, M., Clevers, H., Saftig, P., De Strooper, B., He, X. and Yankner, B. (1998). Destabilization of β-catenin by mutations in presenilin-1 potentiates neuronal apoptosis. *Nature* **395**, 698-702.